JMEPEG (2008) 17:633–643
DOI: 10.1007/s11665-008-9217-5

1059-9495/$19.00

Mathematical Modeling of Pottery Production in Different Industrial Furnaces

Marco Aurelio Ramírez Argáez, Salvador Lucas Huacúz, and Gerardo Trápaga

(Submitted July 26, 2007; in revised form January 10, 2008)

The traditional process for pottery production was analyzed in this work by developing a fundamental mathematical model that simulates the operation of rustic pottery furnaces as employed by natives of villages in Michoacán, Mexico. The model describes radiative heat transfer and fluid flow promoted by natural convection, phenomena that determine the operation of these furnaces. An advanced radiation model called the "Discrete Ordinates Model" was implemented within a commercial computational fluid dynamics software. Process analysis was performed to determine the effect of the design variables on the quality of the pottery pieces and on energy efficiency. The variables explored were: (a) Geometric aspect ratio between diameter and height of the furnace (*D/H*) and (b) Refractory thickness (*L*). The model was validated using experimental temperature measurements from furnaces located in Santa Fe and Capula, Mexico. Good agreement was obtained between experimental and numerically calculated thermal histories. It was found that furnaces with high aspect ratio *D/H* and with thick refractory bricks promote thermal uniformity and energy savings. In general, any parameter that increases the conductive thermal resistance of the wall furnace isolates better, and helps energy savings. Operating conditions that provide the smallest thermal gradients and lowest energy consumption are given.

Keywords heat transfer, natural convection, numerical modeling, pottery furnace, radiation

1. Introduction

Despite the fact that the production of pottery represents an important income to many people in Mexican communities, i.e., it is rather critical for their social and economical status, there are no significant efforts in research and development to improve pottery quality and production for this region. Pottery processing involves several successive stages whatever pottery process is used: (1) Preparation of the mud or clay, (2) Modeling, (3) Drying, (4) Sealing, (5) Decorating, (6) First heating stage, and (7) Second heating stage. Pottery furnaces are normally employed both in the first and second heating stages. Their functions are: (a) Take the modeled and dried mud to a sintered state, where the ceramic body acquires properties such as hardness, stability, mechanical resistance, and chemical resistance to the various physical and chemical external agents. Sintering takes place at a temperature between 700 and 850 °C; sintering is called by the furnace operators as the first heat; and (b) Melting the glass, which is often called "heating of glass," at a temperature range of 980-1000 °C. This melting stage is normally named the second heat. There are several types of furnaces commonly employed by the potters; however, the most popular furnace traditionally used is the "open sky" furnace ("cielo abierto" in Spanish), which is sketched in Fig. 1. Two chambers compose this furnace: (a) a superior chamber where the pieces are placed, and (b) an inferior chamber where combustion of firewood takes place. In order to operate the furnace, handcrafts pieces are introduced to the superior chamber of the furnace, which is covered by a top lid made by refractory pieces, know typically as "tepalcates" (pieces of cooked scrap mud). The furnace starts at low fire and as the operation proceeds, the feeding rate of combustible increases (firewood, charcoal, etc.), to achieve the required final temperatures in the first and second heating stages. The potter empirically estimates adequate temperatures by looking at the color of the pieces, which requires a lot of experience. Temperatures inside the furnace are not measured during a typical heat.

The objective of this work was to develop a rigorous fundamental mathematical model able to assist the design for a better pottery furnace to be used by the potter community. Main features of this furnace must include an optimum performance based on the following considerations: (a) Minimum consumption of energy, (b) Uniform temperature distribution inside the superior chamber, and (c) Propose a furnace configuration that results in optimum heating (location of the burners, geometry of the furnace, and the like). Mathematical modeling was based on complex heat transfer calculations that simulates from first principles in the process of pottery fabrication in a furnace located in Santa Fé de la Laguna (small Indian town in Michoacán State, Mexico located 44.8 km west of Morelia city).

Marco Aurelio Ramírez Argáez, Facultad de Química, Universidad Nacional Autónoma de México (UNAM), Edificio "D", Circuito de los Institutos S/N, Cd. Universitaria, CP 04510, Del Coyoacan, Mexico, D.F., Mexico; **Salvador Lucas Huacúz**, Morelia Institute of Technology, Avenida Tecnológico No. 1500, Col. Lomas de Santiaguito, CP 58120, Morelia, Michoacán, Mexico; and **Gerardo Trápaga**, Centro de Investigación y Estudios Avanzados del IPN, Unidad Querétaro, Libramiento norponiente No. 2000, Fracc. Real de Juriquilla, CP 76230, Santiago de Queretaro, Querétaro, Mexico. Contact e-mail: marco.ramirez@servidor.unam.mx.

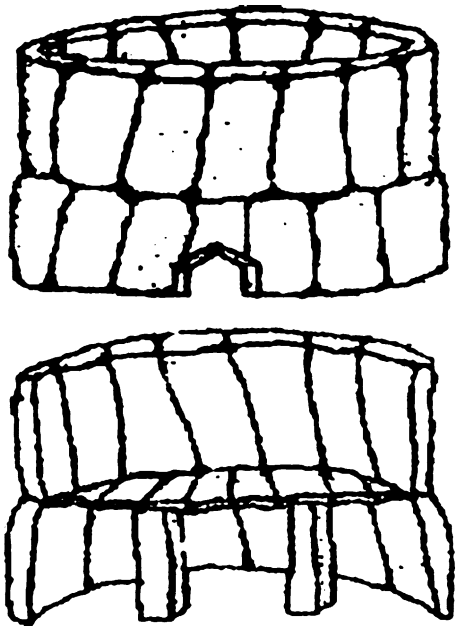

Fig. 1 Schematic representation of cylindrical furnaces opened to sky

Currently, there is not much information about specific research studies on traditional pottery furnaces. Potter communities operate their furnaces empirically. Some of the works that have been made regarding the improvement of the production of pottery, especially in the native regions of Michoacán, México, have been focused to the characterization and preparation of inorganic glasses without lead ("fritas" in Spanish) (Ref 1). Another study was based on the characterization of an inverted draft furnace for ceramics, which was developed at the Santa Fé de la Laguna shop (Ref 2). Project ALFAR (Ref 3) developed a competitive prototype pottery shop. The study of the characterization and preparation of the pastes, from the mineralogical, chemical, and thermal point of view, concluded that in order to obtain pottery handcraft of good mechanical properties it is necessary to optimize the pottery furnace (Ref 4). Specifically regarding studies on pottery furnaces, a "black box" mathematical model (statistical) has been published (Ref 1), describing the thermal history at several positions inside the furnace. The model was developed with measurements made in pottery furnaces located in the México State (Metepec) and Michoacán State (Capula, Patamban, Santa Fé, and Tzintzuntzan) (Ref 1).

2. Mathematical Modeling

2.1 Assumptions and Governing Equations

Traditional pottery furnaces use firewood as the main energy source. Once firewood combines with oxygen contained in the air present in the Inferior chamber, it generates energy by combustion. The energy released is then transferred from the flame to the walls of the furnace, which in turn transfer heat to the pottery pieces by radiation; therefore, inside the superior chamber of the furnace, radiation is the dominant heat transfer mechanism. Consequently, this model tried to represent radiation in the most rigorous way by employing advanced

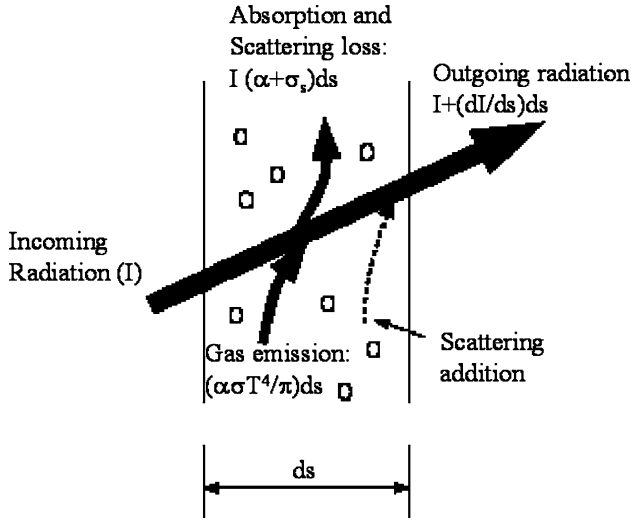

Fig. 2 Schematic representation of the radiation processes occurring in the gas media

radiation models. There are several advanced radiation models available, but after performing an extensive analysis based on the considerations of the optic thickness, convergence, etc. (Ref 5) it was decided to use the so-called "Discrete Ordinates" model (DO) (Ref 6-8), which is already implemented in the commercial Computational Fluid Dynamics (CFD) software FLUENT 6.1. Complex radiation heat transfer calculations were performed inside the furnace considering not only the radiation absorbed and emitted by the walls but also taking into account that the gas in the atmosphere inside the furnace participates in the heat exchange process. The DO model solves the fundamental Radiation Transport Equation, RTE, for a gas media that absorbs, emits, and scatters radiation in the "r" position directed in "s" direction for finite number of discrete solid angles, each of them associated with a vector $\vec{s}$ in a global Cartesian system (x, y, z), which can be written as:

$$\nabla \cdot (I(\vec{r},\vec{s})\vec{s}) + (a+\sigma_s)I(\vec{r},\vec{s}) = an^2\left(\frac{\sigma T^4}{\pi}\right) + \frac{\sigma_s}{4\pi}\int_0^{4\pi} I(\vec{r},\vec{s}')\Phi(\vec{s}\cdot\vec{s}')d\Omega \quad \text{(Eq 1)}$$

where $\vec{r}$ is the position vector, $\vec{s}$ is the direction vector, $\vec{s}'$ is the scattering direction, s is the length of the trajectory, a is the absorption coefficient, σ_s is the scattering coefficient, σ is the Stefan Boltzman coefficient (5.672×10^{-8} W/m^2·K^4), I is total radiation intensity, which depends on the position vector r and the direction s, T is the local temperature, Φ is the phase function, and Ω is the solid angle. The term ($a + \sigma_s$) is the optical thickness or opacity of the gas media. The refraction index n is important when considering radiation in a semitransparent media. Figure 2 illustrates the radiation heat transfer process. It is important to provide a physical interpretation for each one of the terms of Eq 1 within the radiant energy balance: The first term of the left side is the radiation intensity change with respect to the direction coordinate $\vec{s}$, and the second term represents absorption and scattering losses in that direction; while the first term of the right-hand side of the equation is the emission of radiation from air inside the volume element and the second term is the scattering that adds to the radiation intensity I for the same direction.

The scheme of the model is simple: a radiation intensity (I) flows with s direction into the element of volume of gas (with a size ds at a position r). Part of this incoming radiation is absorbed or it is scattered ($I(a + \sigma_s)ds$) by the gas, and the rest goes out in the s direction, i.e., transmitted radiation. Total radiation going out with the same s direction is equal to the transmitted radiation plus the radiation emitted and scattered by the gas in that direction. The DO model requires previous knowledge about the absorption coefficient a as an input datum. The model solves as many transport equations as there are scattering directions $\vec{s}$ considered in the computational domain.

Additionally, the model includes fluid flow phenomena promoted by natural convection driven by temperature gradients inside the furnace (consequently creating density gradients). The fluid flow problem was stated in the laminar regime (see Table 2 where the Grashof number is lower than the transition value from laminar to turbulent regime in flows driven by natural convection) and involves the solution of the Navier-Stokes equations in the r and z components (2D calculation since θ component is not important for symmetric considerations) simultaneously with the continuity equation. The driving force for fluid flow is due to buoyant forces due to gradients in density, which are accounted by the Boussinesq approximation (Ref 9) as an extra source term in the z component of the Navier-Stokes equation.

2.2 Boundary Conditions

Boundary conditions for the energy conservation equation comprise a heat flux coming into the system through the bottom wall (Ref 5). Furthermore, it is necessary to compute heat flux losses through the lateral wall by conduction, which can be achieved only if refractory thickness and its thermal conductivity are known. Actually, the refractory thickness was included as a design parameter in the model, in order to improve energy efficiency of the furnaces. Finally, heat losses through the superior wall by conduction were also used as boundary condition but using a constant thickness of 0.05 m due to the fact that in practice, the superior wall is the worst isolated zone, because it is covered with broken pieces of cooked mud ("tepalcates"). Heat losses by conduction are calculated assuming one-dimensional walls, where heat fluxes can be expressed by Fourier's law as:

$$\vec{q}_x = -k\frac{dT}{dx} \qquad \text{(Eq 2)}$$

where q_x is the heat flux by conduction through the furnace walls, k is thermal conductivity of the wall refractory, and x is the coordinate perpendicular to the wall since it is assumed that one-dimensional heat conduction is directed perpendicular to each wall.

For the fluid flow problem, the boundary conditions are quite simple and indicate the nonslip condition at the walls which means that parallel components of velocity to the walls are zero, while it is also considered that walls are impermeable to air, meaning that normal components of velocity to the wall surface are also zero.

Runs were performed in unsteady state from an initial condition of constant ambient temperature marching with time until the end of the heat is reached at 11,700 s of operation.

2.3 Solution

The complete set of partial differential equations that describe the radiation heat transfer problem using the "DO" model together with two components of the Navier-Stokes equations plus the continuity equation subjected to their proper boundary conditions were cast into a numerical finite element formulation that is already implemented in the commercial software for computational fluid dynamics FLUENT version 6.1. The grid employed for this computation used 15,500 nodes in a uniform grid after an extensive grid sensitivity study (Ref 5). Time steps of 1 s were used in all simulations.

2.4 Validation of the Model with Experimental Measurements at Santa Fé, Mich. and Capula, Mich.

There is a study found in the literature (Ref 1) that performed experimental measurements of thermal histories during operation of real pottery furnaces at Santa Fé and Capula, Michoacán. Table 1 reports dimensions of these furnaces (diameter, height, refractory thickness, total area of radiation, furnace volume), firewood consumption, energy generation rate, duration of each heat, and average heat fluxes or heat flows, while in Table 2 physical and transport properties for air are presented.

It is noted that we know the total energy produced when a kilogram of firewood is burned in air, but the way this energy is released with time it is not known. We arrived to the conclusion that the amount of heat flowing into the furnace is equal to the energy produced by combustion of firewood (see Table 1) per unit of area of the bottom wall, but distributed in time as a

Table 1 Operating conditions of Santa Fé and Capula furnaces

Properties	Santa Fé	Capula
Height	0.55 m	0.853 m
Diameter	0.62 m	1.1 m
Area	0.95033 m^2	2.1904 m^2
Volume	0.59921 m^3	2.4094 m^3
Thickness of refractory	0.15 m	0.20 m
Wood consumption	112 kg	143 kg
Total time	11,700 s	21,600 s
Energy consumption	1.94×10^9 J	2.48×10^9 J
Average heat flow	165811.966 W	1.15×10^5 W
Total heat flux	174,478 W/m^2	5.23×10^4 W/m^2
Heat flux as a function of time	$q(t) = 0.63253 \times (23400 - t)t$	$q(t) = 1.673\times 10^5 e^{-\frac{1}{2}\left(\frac{t-21600}{5400}\right)^2}$

Table 2 Physical properties of air

Gas properties (air)	Santa Fé (T = 1147 K)	Capula (T = 1142 K)
Boussinesq's reference density	0.259 kg/m^3	0.2605 kg/m^3
Specific heat	1180 J/kg·K	1170 J/kg·K
Thermal conductivity	0.0756 W/mK	0.0753 W/mK
Viscosity	4.56×10^{-5} kg/m·s	4.55×10^{-5} kg/m·s
Thermal expansion coefficient	8.22×10^{-4} K^{-1}	8.54×10^{-4} K^{-1}
Raleigh number (Ra)	1.4166×10^9	1.3723×10^9
Prandtl number (Pr)	0.7301	0.6525
Grashof number (Gr)	1.03426×10^9	8.95425×10^8

polynomial function of time. These polynomial distributions are dictated by the shape of the experimentally determined thermal histories. This heat flux is distributed uniformly along the bottom wall. In other words, based on the shape of the measured temperature histories, the heat flux entering the furnace was distributed in time in such a way that this flux has similar function of time (in shape) as the measured thermal histories, but with the constraint that integration of the heat flux distribution over the total time and bottom area gives the total energy generated by the combustion of the total amount of firewood employed. Finally, physical properties recently measured for the refractory are reported in Table 3 (Ref 4).

Figure 3(a) shows the experimental setup and the position of each thermocouple inside furnace. The thermocouple T1 is highlighted because thermal histories at that position were employed to validate our numerical model for the Santa Fé and de Cápula furnaces, while in Fig. 3(b) and (c) comparisons between experimental (dots) and numerically calculated results (solid lines) are presented. These figures show excellent agreement between experiments and numerical predictions, which constitutes by itself the validation of our model.

Table 3 Physical properties of the refractory material

Properties	Refractory of Santa Fé furnace	Refractory of Capula furnace
Thermal diffusivity, m^2/s	1.23×10^{-7}	1.5×10^{-7}
Density, kg/m^3	1.98×10^{3}	1.74×10^{3}
Thermal conductivity, W/mK	1.031	1.65
Specific heat, J/kg·K	4233.39	6.32×10^{3}

3. Results and Discussion

Process analysis was carried out to understand the performance of Santa Fé's furnace (dimensions, amount of firewood, etc). This process analysis was focusing on exploring the effect of the following design variables on the productivity, energy efficiency, and thermal uniformity of the furnace: (1) Aspect ratio of the superior chamber of the furnace, i.e., diameter over height (*D*/*H*) and (2) Wall refractory thickness. Outputs obtained for each design variable were: (1) Temperature distribution at the end of the heat; (2) Flow patterns promoted by natural convection; (3) Thermal history of thermocouple T1 (see Fig. 3a); (4) Usable volume fraction of the furnace. The last parameter refers to the region inside the superior chamber of the furnace where temperature ranges from 1260 to 1280 K, which corresponds to the best temperature range for pottery production according to the potter expertise (especially in the second heating stage). Regions where temperatures at the end of the heat are out of this range are not suitable for good quality pottery fabrication; and (5) Maximum temperature gradients inside the furnace as a function of time, i.e., T1-T7 (see Fig. 3a).

3.1 Effect of the Aspect Ratio (D/H)

For this analysis, the volume of the superior chamber of the furnace was kept constant and the aspect ratio *D*/*H* values used in this analysis were 1.75 (case 1), *D*/*H* = 0.5 (case 2), *D*/*H* = 1 (case 3), and *D*/*H* = 2.5 (case 4). All cases were run with a refractory thickness of 0.15 m and the heat flux distribution entering from the bottom wall as a function of time is reported in Table 1.

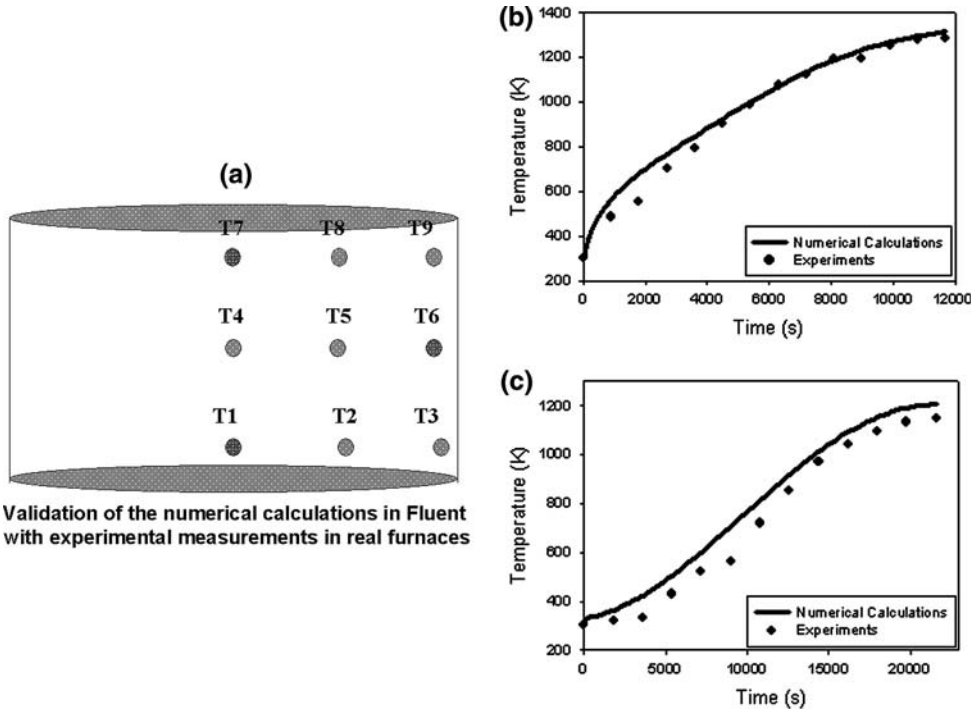

Fig. 3 (a) Experimental positions of the several thermocouples in both furnaces. (b) Experimental and calculated temperature profiles as a function of time in a production heat in the furnace of Santa Fé. (c) Experimental and calculated temperature profiles as a function of time in a production heat in the furnace of Capula

Temperature distribution at the end of the operation can be seen in Fig. 4(a-d) for the different aspect ratios studied in this work. From the results it is evident that by decreasing the aspect ratio D/H, temperature gradients increase between the hottest zone close to the bottom and the coolest zone near the top surface. In the furnace with an aspect ratio $D/H = 2.5$ (Fig. 4d) it can be appreciated that temperatures are more uniformly distributed than in any other case. Besides, temperatures obtained at the end of the heat are higher in most of the volume of the Santa Fé's furnace with an aspect ratio D/H of 2.5 than in any furnace with lower aspect ratios. These two facts mean that the aspect ratio is a very important design parameter for the efficiency in pottery production since the higher is the aspect ratio D/H of the furnace, the lower is the temperature gradients and the better is the uniformity of temperatures inside the furnace. Even more importantly, the better is the energy efficiency since for the same amount of energy employed higher temperatures are obtained at the same final time for a $D/H = 2.5$ than in any other D/H value. This would imply the possibility of using the entire volume of the furnace to allocate pottery handcraft since the bottom and top of the superior chamber would be practically at the same temperature, which would avoid wastes of material due to pieces not sintered or exposed too much at high temperatures. This in turn would mean an improvement in productivity and energy savings since less time and energy would be required to reach the appropriate range of temperatures for pottery fabrication. The benefits of operation with $D/H = 2.5$ do not occur in furnaces with low values of D/H (for example $D/H = 0.5$ in Fig. 4b), where pieces located at the top of furnace would be at a temperature 500 °C less than the pieces located at the bottom of the furnace. Such a pronounced temperature gradient inside the furnace (for low D/H values) would cause that pottery located at the top would have very different physical properties than those located at the bottom of the furnace, and consequently some pieces would not sinter while others would be sintered for more time than necessary, increasing dramatically the number of rejected pieces. However, there is a technical difficulty in building furnaces with high values of D/H, since it would be very difficult to distribute the heat flux evenly over the entire large bottom area of the superior chamber. Probably, a simple solution would be to

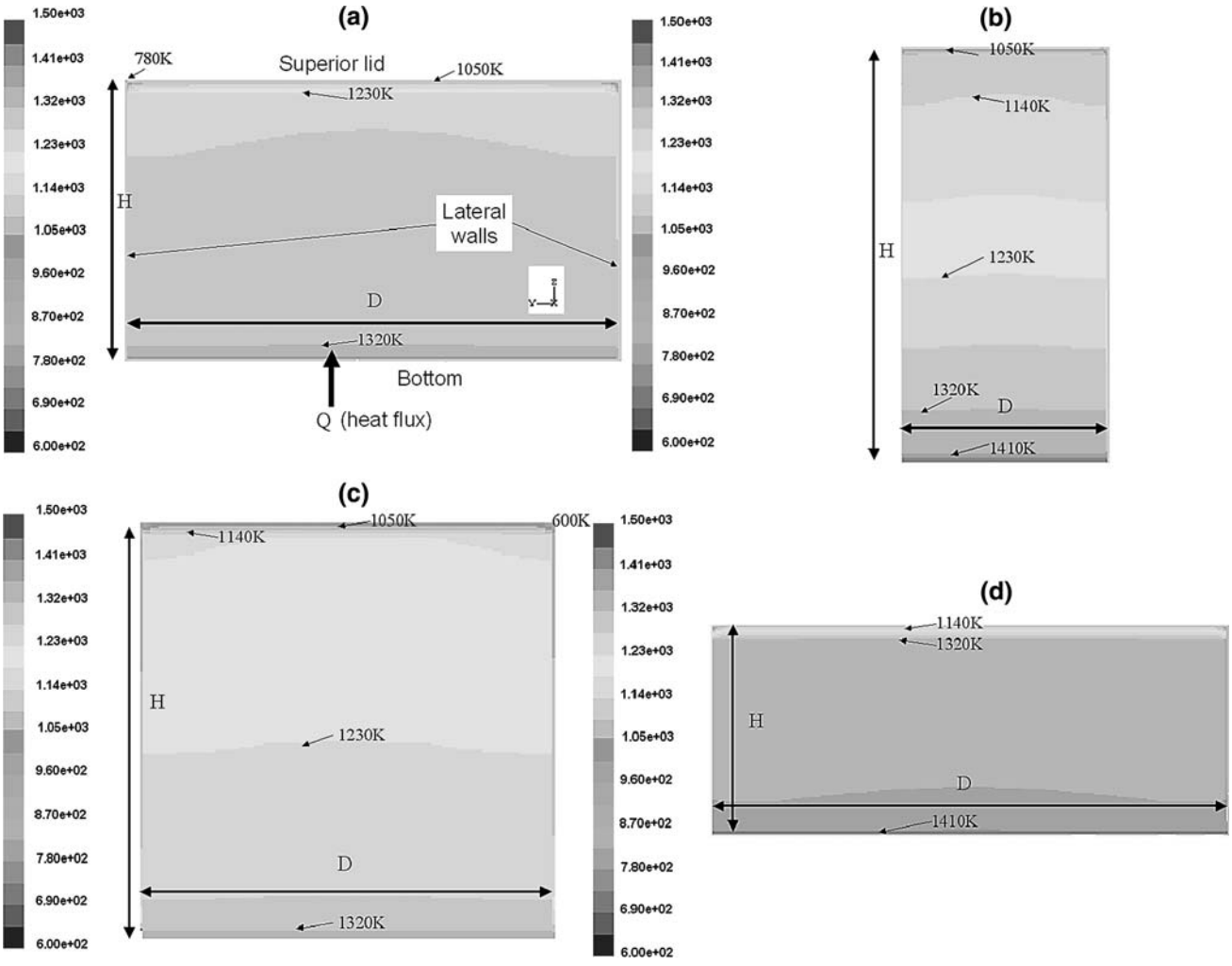

Fig. 4 Calculated temperature contours at the end of the heat in the furnace located in Santa Fé using the same refractory, same volume of the chamber, and the same amount and feeding rate of firewood, but varying the aspect ratio D/H: (a) $D/H = 1.75$ (actual aspect ratio of the furnace), (b) $D/H = 0.5$, (c) $D/H = 1$, and (d) $D/H = 2.5$

replace firewood as energy source by gas burners, which are ideal to regulate and control heat flows easily.

Flow patterns obtained at the end of the heat are depicted in Fig. 5(a-d) for each furnace with different aspect ratios *D/H* explored in this work. Flow patterns are promoted by natural convection since there is no other force driving the flow inside the furnace. Natural convection results from the existing thermal gradients. Air at low temperatures is less dense than hot air; therefore, due to the heating of the superior chamber of the furnace through the bottom surface, hot air (with low density) is under cold air (with high density), as can be appreciated from the temperature contours of Fig. 4. This physical condition is unstable and thus cold air will descend close to the side walls while hot air ascends vertically through the center of the furnace. This circulation scheme forms a recirculation path since there is no way for the air to escape through the furnace due to the impermeability of the walls. In the four cases of Fig. 5(a-d), two recirculation loops can be easily identified due to the system symmetry. These flow patterns present moderate velocities of the order of 0.1 m/s, which corresponds to a typical value for flows driven by natural convection due to thermal gradients. Velocities will be greater in magnitude as temperature gradients increase inside the furnace. Therefore, the furnace with aspect ratio *D/H* = 0.5 has larger thermal gradients(see Fig. 4b, 5b), presenting higher magnitudes of air velocity than in the other cases with higher *D/H* values. Particularly, a furnace with the largest aspect ratio of *D/H* = 2.5, which has a uniform temperature distribution (small thermal gradient), presents the weakest flow patterns, i.e., air is more static in furnaces with *D/H* = 2.5. However, natural convection does not play a key role in the heat transfer process, since, in this case, convection heat transfer can be neglected in comparison with radiation. Performing a simple order of magnitude analysis, it can be concluded that natural convection with velocities in the order of 0.1 m/s typically are associated with heat transfer coefficients lower than 3 $W/m^2 \cdot K$ (Ref 10). Estimation of radiative heat flux is of the order of 10^5 W/m^2, while for convective heat flux is of the order of 10^3 W/m^2 for this system. This is the reason why the flow pattern by itself is an unimportant phenomena for the operation of the furnace, since convection as a heat transfer mechanism is unimportant relative to radiation.

Temperature profiles in the furnace obtained at the end of the heat from 1260 to 1280°K can be seen in Fig. 6(a-d) for each furnace and different aspect ratios. These plots have practical importance because the range of temperatures shown (1260-1280°K) is considered to be the optimum in order to obtain good quality pieces. Otherwise, pieces maintained at

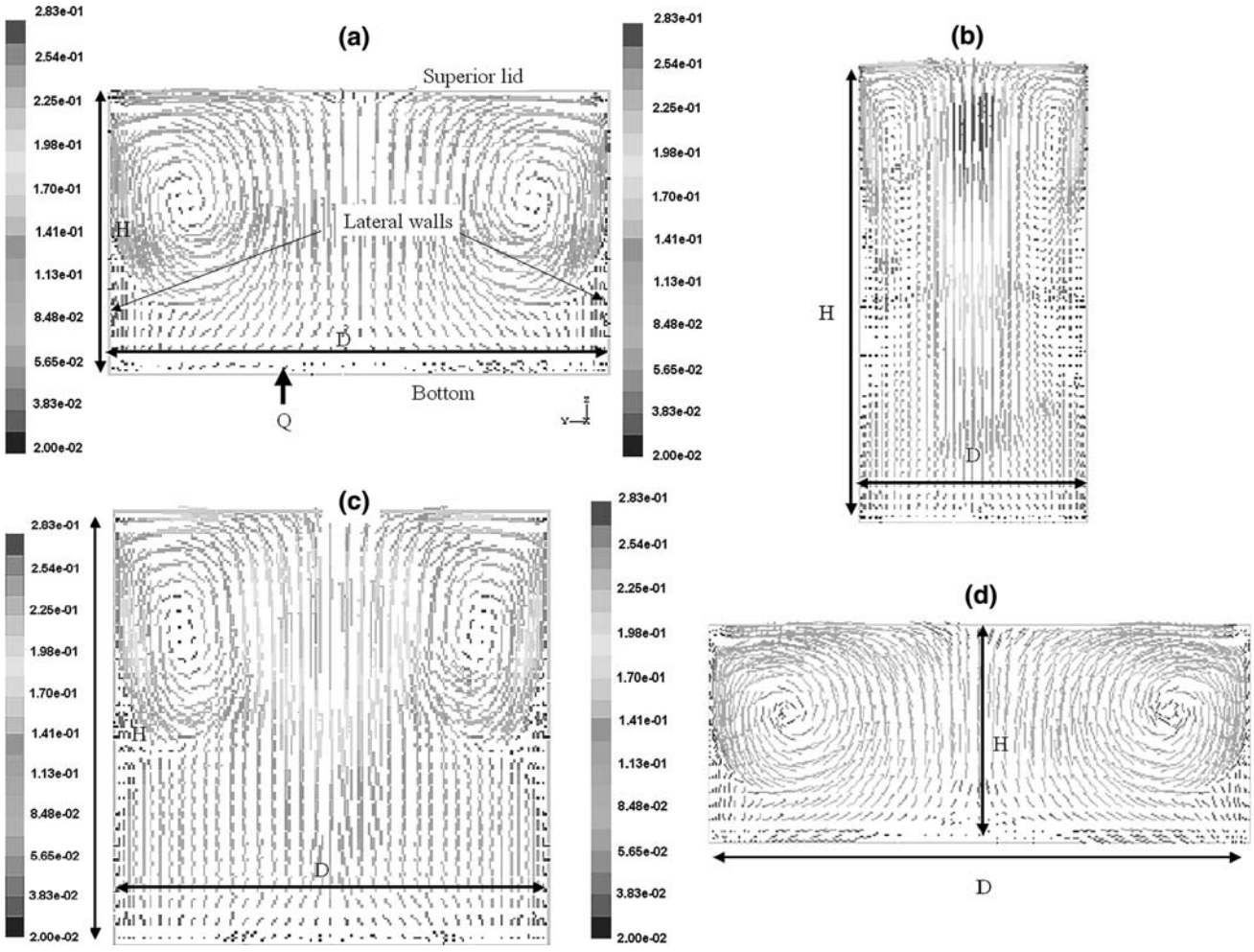

Fig. 5 Calculated velocity profiles of air inside the furnace (natural convection) at the end of the heat in the furnace located in Santa Fé using the same refractory, the same volume of the chamber, and the same amount and feeding rate of firewood, but varying the aspect ratio *D/H*: (a) *D/H* = 1.75 (actual furnace), (b) *D/H* = 0.5, (c) *D/H* = 1, and (d) *D/H* = 2.5

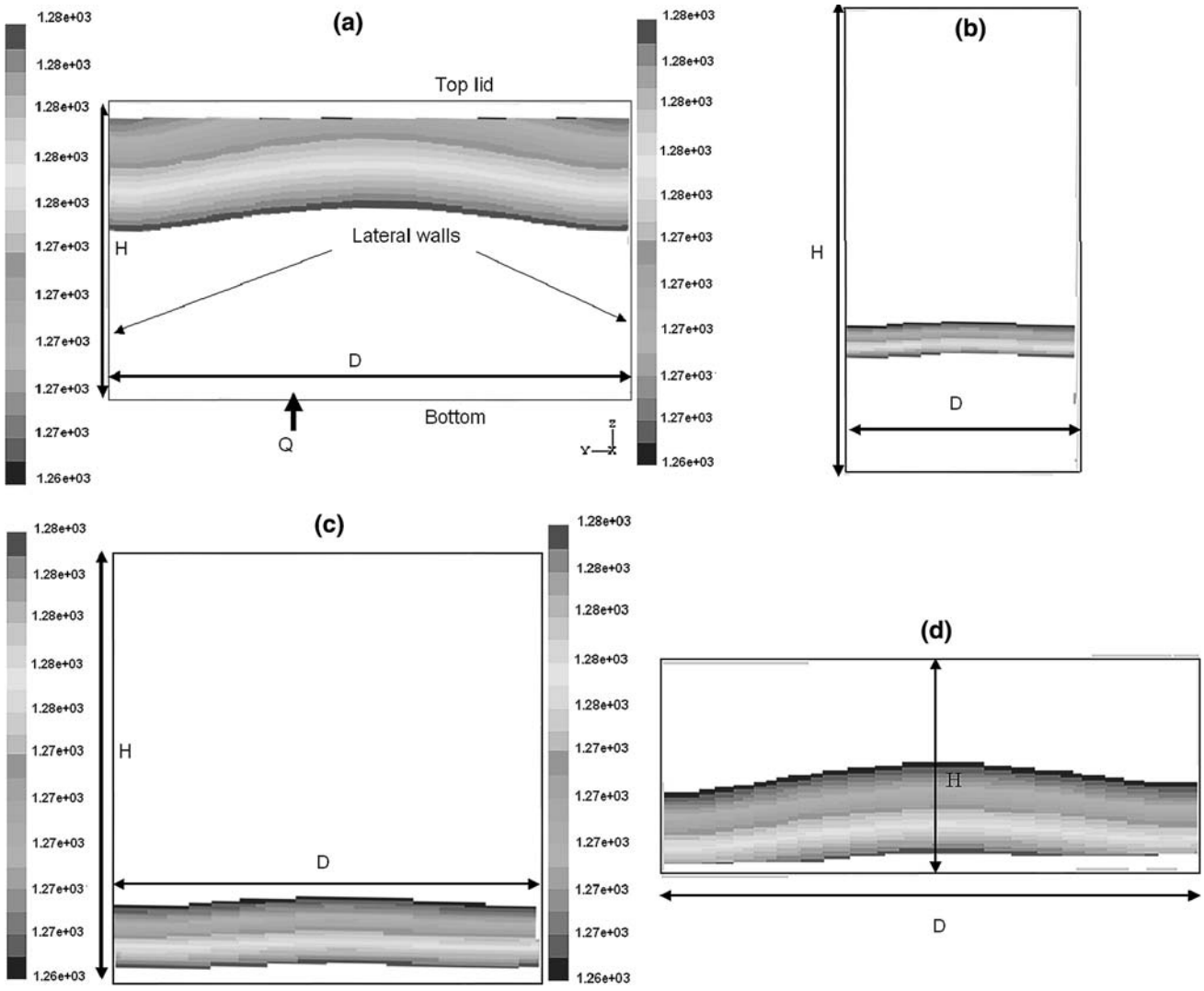

Fig. 6 Calculated temperature profiles inside the furnace at the end of the heat showing the fraction of the furnace located in Santa Fé able to produce good quality pottery (1260-1280 K), using the same refractory, the same volume of the chamber, and the same amount and feeding rate of firewood, but varying the aspect ratio *D/H*: (a) *D/H* = 1.75 (actual furnace), (b) *D/H* = 0.5, (c) *D/H* = 1, and (d) *D/H* = 2.5

temperatures above or below this temperature range will not accomplish the minimum quality criteria based on physical and mechanical properties, resulting in disposal of pieces. Consequently, temperature contours plotted from 1260 to 1280 K are used as the criteria to specify the usable volume fraction of the furnace, since these contours give us a clear and graphic indication of the best region to allocate pottery in the furnace. Evidently, furnaces with low aspect ratio *D/H* have a small useful region than a furnace with high aspect ratio (*D/H* = 2.5), which has the biggest fraction of the volume useful for obtaining good quality handcrafts. This is in complete agreement with previous comments regarding internal thermal gradients, i.e., a furnace with large thermal gradients cannot provide high useful volume of the furnace when compared against a furnace presenting a uniform temperature distribution. Therefore, the higher the aspect ratio is, the higher the thermal uniformity and the bigger the volume fraction of the furnace useful for locating pieces are, because these pieces will be subjected to the same adequate temperature.

Computed thermal histories near the center and at the bottom of the furnace (thermocouple T1 in Fig. 3a), as well as the maximum thermal gradient inside the furnace predicted by the model (T1-T7 from Fig. 3a) are presented in Fig. 7(a) and (b), respectively. From the thermal history presented in Fig. 7(a), it can be observed that the furnace with the lowest aspect ratio (*D/H* = 0.5) presents a slightly higher heating rate than that for the rest of the cases. However, at the end of the heat (more than 11,000 s) it can be seen that the trend is somewhat inverted. This means that despite the fact that the same amount of heat is introduced through the bottom during the same time, furnaces with larger *D/H* present better thermal efficiency. Without doubt this is due to the great bottom surface area (through which heat flows into the furnace) associated to *D/H* and at the same time small lateral areas that are associated to heat losses. The opposite happened with furnaces with low aspect ratios *D/H*, with big lateral surface areas through which enormous heat losses occur. It is recognized that larger conduction area means less thermal resistance and therefore more heat losses are present and less energy efficiency is achieved in the operation of the furnace.

Regarding the maximum temperature gradients inside the furnace (see Fig. 7b), it can be appreciated that as *D/H*

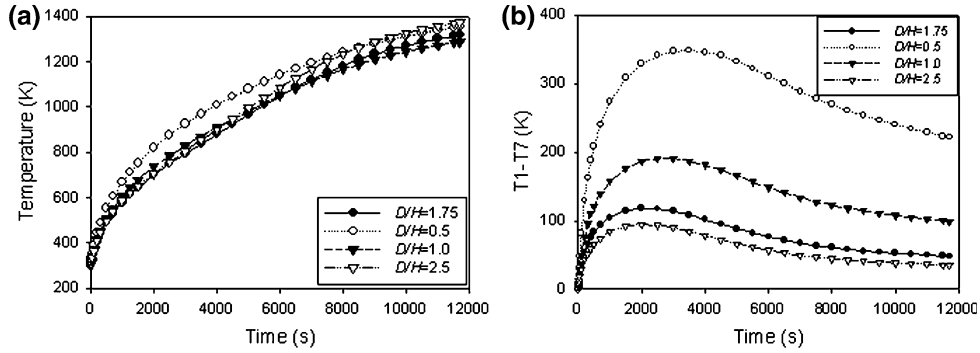

Fig. 7 (a) Thermal history at the position of thermocouple number 1 inside the furnace of Santa Fé, using the same refractory, the same volume of the chamber, and the same amount and feeding rate of firewood, but varying the aspect ratio D/H (D/H = 1.75 (actual furnace), 0.5, 1.0, and 2.5). (b) Maximum thermal gradient history (T1-T7) inside the furnace of Santa Fé using the same refractory, the same volume of the chamber, and the same amount and feeding rate of firewood, but varying the aspect ratio D/H (D/H = 1.75 (actual furnace), 0.5, 1.0, and 2.5)

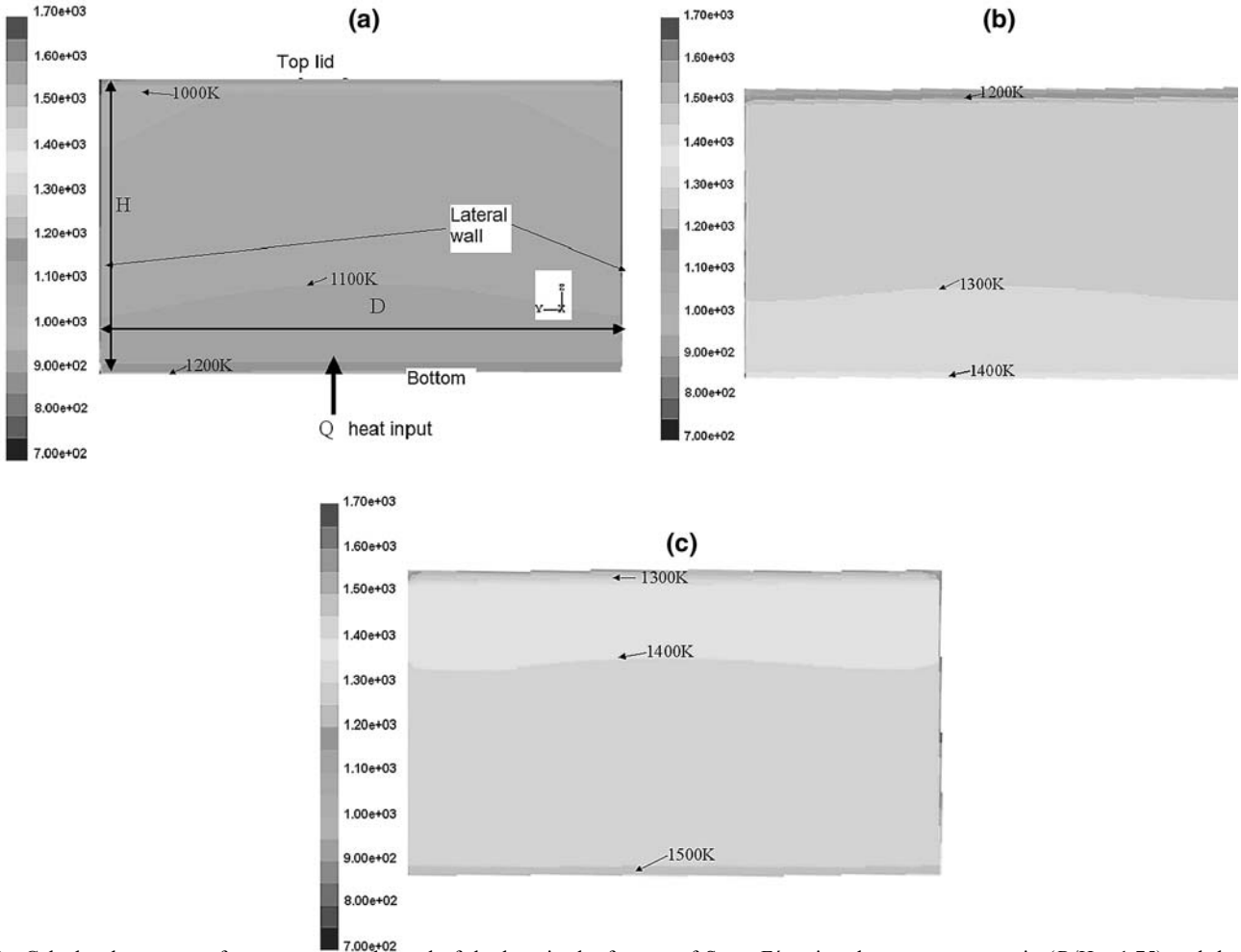

Fig. 8 Calculated contours of temperature at the end of the heat in the furnace of Santa Fé, using the same aspect ratio (D/H = 1.75) and the same amount and feeding rate of firewood, but varying thickness of the refractory: (a) L = 0.05 m, (b) L = 0.15 m (actual furnace), and (c) L = 0.25 m

increases the thermal gradient decreases. It is interesting to note that the thermal gradient increases with time from the beginning and then reaches a maximum that occurs at longer times as D/H decreases and then the gradient decreases with time. Another interesting aspect to note is the high maximum thermal gradient reached in the furnace with D/H = 0.5 of approximately 350 °C in contrast to the thermal difference of only 90 °C reached in the furnace with D/H = 2.5. This result is in excellent agreement with the statements about temperature profiles given above.

3.2 Effect of the Thickness of Refractory

In these calculations, the furnace aspect ratio was kept constant at $D/H = 1.75$ (actual furnace value) and the heat flux distribution with time entering the furnace through the bottom was the same as reported in Table 1. Refractory thickness values used in this study were 0.05, 0.15 (thickness of lateral and bottom walls in the actual furnace), and 0.25 m. Temperature profiles inside the furnace at the end of the process can be seen in Fig. 8(a-c), for the three furnaces with different wall thickness explored in this work. It can be noted that as the refractory thickness is increased the final temperatures inside the furnace increase for the same amount of energy supplied and for the same time. When a refractory with thickness of 0.05 m is used, the average temperature inside the furnace at the end of the process is between 1000 and 1100 K, which would be quite low and hence the operation would require more time and energy consumption to reach the adequate temperatures for pottery production. On the contrary, when a refractory 0.15 m thick is used, the average temperature at the end of a normal heat (11,700 s) is between 1200 and 1300 K, while using a thicker refractory brick of 0.25 m, the average temperatures at 11,700 s are above 1400 K. An explanation for these results is evident since the thicker refractory isolates better the furnace and the energy transferred from the combustion of firewood is more efficiently used. A thermal resistance by conduction in a one-dimensional wall, which opposes to the heat transfer (obviously the higher the thermal resistance the lower is the heat flow through the furnace walls), can be defined as:

$$\text{Thermal Resistance} = \frac{L}{kA} \qquad \text{(Eq 3)}$$

where L is the refractory thickness, A is the heat transfer area, and k is the thermal conductivity of the wall. The thermal conductivity k should be the same due to the opposition of the Indian potter community to substitute their furnaces made of adobe bricks obtained from local clays (same k), compared to any other commercial clay having much lower thermal conductivity and consequently being a better insulation. This is why the only design variables to be changed in this study are A (through the aspect ratio D/H) and L. Obviously, by maintaining constant the aspect ratio D/H, A did not change in these calculations (it was stated in the previous section that a decrement in D/H increases A and also increases the heat losses and efficiency decreases), then the refractory thickness being the only design variable in this section. Then, an incre-

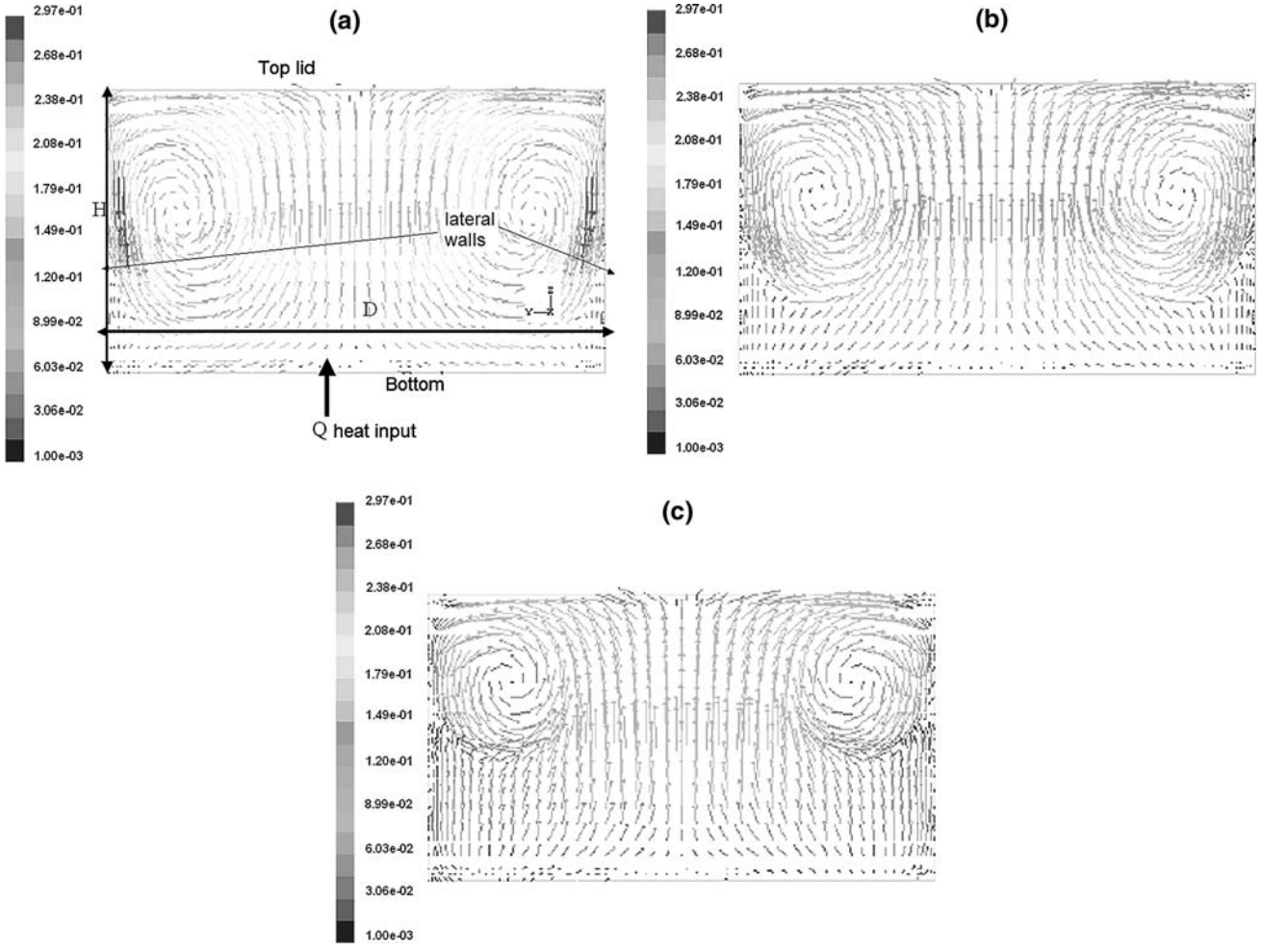

Fig. 9 Calculated velocity profiles inside the furnace of Santa Fé (natural convection) at the end of the heat, using the same aspect ratio ($D/H = 1.75$) and the same amount and feeding rate of firewood, but varying thickness of the refractory: (a) $L = 0.05$ m, (b) $L = 0.15$ m (actual furnace), and (c) $L = 0.25$ m

ment in the thickness of refractory increases the thermal resistance by conduction and then thicker refractory walls insulate better the furnace improving energy efficiency by minimizing heat losses.

Flow patterns at the end of the heat in different furnaces with varying thickness of refractory are shown in Fig. 9(a-c). It is clearly seen from the figures that increasing the thickness of the refractory decreases the intensity of the convective streams (velocity vectors are larger close to the lateral walls in Fig. 9a than in Fig. 9b, c), which is due to the smaller thermal gradients associated with thicker walls (more uniform temperatures in the furnace).

Temperature profiles at the end of the operation from 1260 to 1280°K can be seen in Fig. 10(a-c) for the three furnaces employing different refractory wall thickness. It was already stated that plotting this temperature range (1260-1280 K) is a good graphic indicator of the useful region inside the superior chamber of the furnace. In this case, the total operating time was controlled to allow all furnaces to reach the mentioned proper range of temperatures (evidently more energy was introduced into the furnace or more actual time took the operation as the refractory becomes thinner). It can be noted that there are no significant differences regarding the useful zones of the three cases varying refractory thickness, being slightly bigger for thicker walls of 0.25 m than for thinner walls. Additionally, the strip of useful volume fraction looks more horizontal than in the other cases, because the heat losses are lower when wall thickness is L = 0.25 m, while for cases with thickness of 0.05 and 0.15 m the useful strip region has the shape of an arc due to the great heat losses through lateral walls. However, it is necessary to remember that the total energy input was higher as the refractory thickness becomes thinner.

Computed thermal histories at the center bottom of the furnace (thermocouple T1) and maximum gradient of temperatures as a function of time can be seen in Fig. 11(a) and (b), respectively. It can be observed from Fig. 11(a) that as the walls get thicker temperatures get hotter at a given time (the energy input being the same at a given time for each case). This confirms that thicker walls improve energy efficiency since heat losses are inversely proportional to the wall thickness (Eq 3). Regarding thermal gradients inside the furnace, the thicker the walls the lower is the gradient. However, the thermal gradients in the furnace are more sensitive to the furnace aspect ratio than to the thickness of the refractory, since the maximum thermal gradient reached for a wall thickness of 0.05 m is 130 °C, while using a thickness of 0.25 m maximum gradient reached is 110 °C, i.e., the wall thickness do not influences thermal uniformity but it is very important on energy efficiency. It is not simple to give a fully comprehensive reason of why the wall thickness doesn't determine the thermal gradients in the furnace, but it seems that the aspect ratio is the design variable

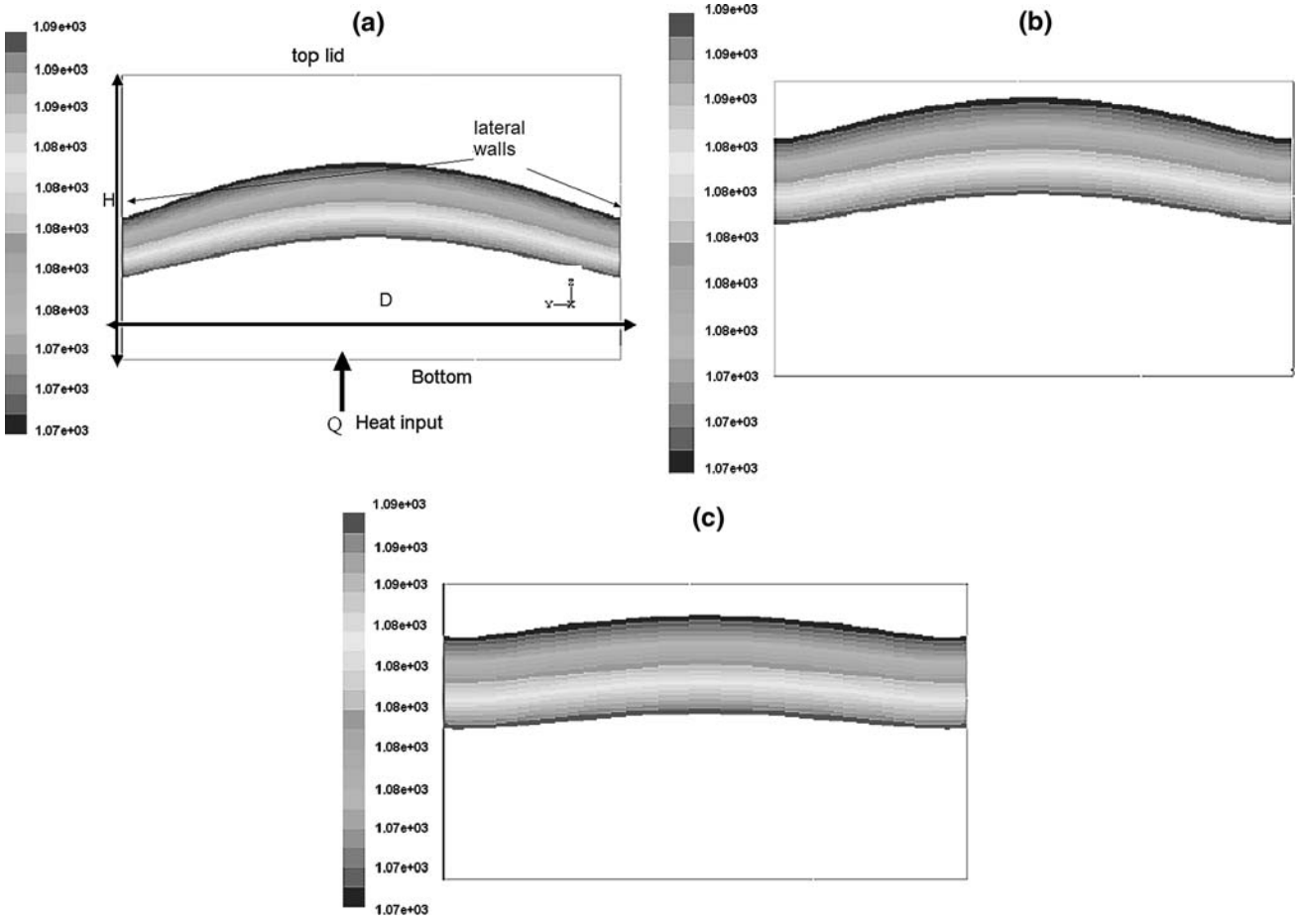

Fig. 10 Calculated temperature profiles inside the furnace of Santa Fé at the end of the heat showing the fraction of the furnace able to produce good quality pottery (1260-1280 K), using the same aspect ratio (D/H = 1.75) and the same amount and feeding rate of firewood, but varying thickness of the refractory: (a) L = 0.05 m, (b) L = 0.15 m (actual furnace), and (c) L = 0.25 m

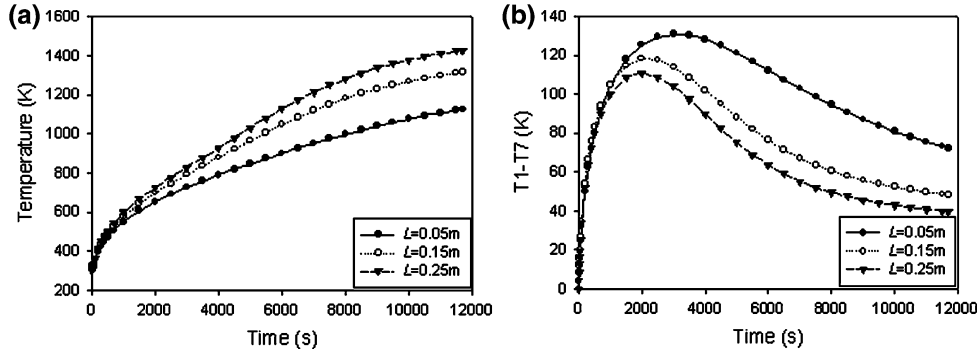

Fig. 11 (a) Thermal history at the position of thermocouple number 1 inside the furnace of Santa Fé, using the same aspect ratio (D/H = 1.75), the same volume of the chamber, and the same amount and feeding rate of firewood, but varying thickness of the refractory L (L = 0.05 m, L = 0.15 m (actual furnace), and L = 0.25 m). (b) Maximum thermal gradient history (T1-T7) inside the furnace of Santa Fé using the same aspect ratio D/H = 1.75, the same volume of the chamber, and the same amount and feeding rate of firewood, but varying thickness of the refractory L (L = 0.05 m, L = 0.15 m (actual furnace), and L = 0.25 m)

controlling uniformity, indicating that radiation between surfaces and the size of the lateral walls both play key roles regarding heat losses. Therefore, having big hot surface area at the bottom and small lateral walls help to homogenize temperatures inside the furnace, and to save energy.

4. Conclusions

In this work the operation of traditional adobe furnaces employed to produce pottery that are currently operating in some villages located in Michoacán, México was analyzed. The main objective of the present research was to provide optimum design conditions in order to achieve adequate energy efficiency, high productivity, and pottery of good quality. The design parameters investigated in this work were: (a) Geometric aspect ratio (D/H), and (b) Thickness of the refractory (L). Based on the results obtained from the model it was found that: (a) furnaces with increasing values of the aspect ratio (D/H) are better than furnaces with small aspect ratio. High aspect ratio furnaces promote thermal uniformity and energy savings since the higher is the aspect ratio the higher is the area where heat transfer takes place from the bottom where firewood is located and simultaneously decreases lateral wall through which there are heat losses. Then, by decreasing the area through which there are heat losses automatically increases the thermal resistance and consequently the furnace is better isolated. However, it is difficult to heat more area since it is necessary to distribute better the firewood across the combustion chamber, implying that it is not likely to operate under such aspect ratios where furnace diameter is very large unless it were possible to introduce the heat flow by using natural gas that can be easily directed by a simple pipe system with burners. (b) Furnaces employing thicker refractory walls work better than furnaces with thin refractory walls. This is due to the fact that increasing the refractory thickness improves thermal resistance by conduction through the walls, meaning that furnaces are better isolated, and consequently they can achieve better thermal uniformity and energy savings. However, there is a physical limit for the refractory thickness after which it would be impossible to construct the furnace, since the resulting bricks would not be adequate to the architecture and building of the furnace. The refractory type is another variable that can further improve the thermal behavior of these furnaces, since using better insulating materials would improve its operation. However, we decided not to explore this variable because, in our opinion, it is very important to employ clays found near the villages, since, in the contrary case, native communities would not accept the bricks because it would go against their traditions and it would increase the cost of the furnace.

Acknowledgment

We would like to thank the Mexican Council of Science and Technology (CONACYT) for the financial support given to this research through the project J36166-U.

References

1. L. Rojas, Desarrollo de un vidriado sin plomo a baja temperatura para alfarería tradicional (Development of a Glasses Without Lead at Low Temperature for Traditional Pottery), Chemical Engineering Thesis, Universidad Autónoma Metropolitana, México, 1995
2. J. Navia and J.S. Ochoa, *Caracterización de un Horno de Tiro Invertido para Cerámica*. Grupo Interdisciplinario de Tecnología Rural Apropiada (GIRA), Michoacán, México, 1999
3. ALFAR: Boletín Informativo No. 1, May-July, Morelia, Michoacán, México, 1996
4. L. Huacúz, *Medición de Propiedades Térmicas, Mecánicas y Químicas de las Arcillas de Santa Fe Utilizadas en la Alfarería*. Universidad Michoacana de San Nicolás de Hidalgo, Michoacán, México, 1999
5. S.L. Huacúz, Modelación matemática de la operación de hornos para la alfarería en el estado de Michoacán (Mathematical Modeling of the Operation of Pottery Furnaces in the State of Michoacán), Master's Thesis, Morelia Institute of Technology, Mexico, 2004
6. G.D Raithby and E.H. Chui, A Finite-Volume Method for Predicting a Radiant Heat Transfer in Enclosures with Participating Media, *J. Heat Transfer*, 1990, **112**(2), p 415–423, in English
7. K. Stammes and R.A. Swanson, A New Look at the Discrete Ordinate Method for Radiative Transfer Calculations in Anisotropically Scattering Atmospheres, *J. Atmos. Sci.*, 1981, **38**(2), p 387–299, in English
8. W.A. Fiveland, Discrete Ordinate Methods for Radiative Heat Transfer in Isotropically and Anisotropically Scattering Media, *J. Heat Transfer*, 1987, **109**(3), p 908–812, in English
9. J. Szekely, *Fluid Flow Phenomena in Metals Processing*, 1st ed., Academic Press Inc., 1979, p 183–189
10. F.P. Incropera, D.P. Dewitt, *Fundamentals of Heat and Mass Transfer*, 5th ed., John Wiley, 2001, p 8–9